



**University of
Sunderland**

Huang, Chenxi, Lan, Yisha, Chen, Sirui, Liu, Qing, Luo, Xin, Xu, Gaowei, Zhou, Wen, Lin, Fan, Peng, Yonghong, Ng, Eddie Y. K., Cheng, Yongqiang, Zeng, Nianyin, Zhang, Guokai and Che, Wenliang (2019) Patient-Specific Coronary Artery 3D Printing Based on Intravascular Optical Coherence Tomography and Coronary Angiography. *Complexity*, 2019 (571259). pp. 1-10. ISSN 1076-2787

Downloaded from: <http://sure.sunderland.ac.uk/id/eprint/11518/>

Usage guidelines

Please refer to the usage guidelines at

<http://sure.sunderland.ac.uk/policies.html> or alternatively contact sure@sunderland.ac.uk.

Research Article

Patient-Specific Coronary Artery 3D Printing Based on Intravascular Optical Coherence Tomography and Coronary Angiography

Chenxi Huang ¹, Yisha Lan,² Sirui Chen,² Qing Liu,¹ Xin Luo,² Gaowei Xu,² Wen Zhou,³ Fan Lin ¹, Yonghong Peng ⁴, Eddie Y. K. Ng ⁵, Yongqiang Cheng ⁶, Nianyin Zeng ⁷, Guokai Zhang ⁸ and Wenliang Che ⁹

¹School of Informatics, Xiamen University, Xiamen, China

²Department of Computer Science and Technology, Tongji University, Shanghai, China

³School of Computer and Information, Anhui Normal University, Wuhu, China

⁴Faculty of Computer Science, University of Sunderland, Sunderland, UK

⁵School of Mechanical and Aerospace Engineering, Nanyang Technological University, 639798, Singapore

⁶School of Engineering and Computer Science, University of Hull, Hull HU6 7RX, UK

⁷Department of Instrumental and Electrical Engineering, Xiamen University, Xiamen, China

⁸School of Software, Tongji University, Shanghai, China

⁹Department of Cardiology, Shanghai Tenth People's Hospital, Tongji University School of Medicine, Shanghai, China

Correspondence should be addressed to Nianyin Zeng; zny@xmu.edu.cn, Guokai Zhang; zhangguokai_01@163.com, and Wenliang Che; chewenliang@tongji.edu.cn

Received 1 August 2019; Accepted 26 November 2019; Published 23 December 2019

Academic Editor: Xinggang Yan

Copyright © 2019 Chenxi Huang et al. This is an open access article distributed under the Creative Commons Attribution License, which permits unrestricted use, distribution, and reproduction in any medium, provided the original work is properly cited.

Despite the new ideas were inspired in medical treatment by the rapid advancement of three-dimensional (3D) printing technology, there is still rare research work reported on 3D printing of coronary arteries being documented in the literature. In this work, the application value of 3D printing technology in the treatment of cardiovascular diseases has been explored via comparison study between the 3D printed vascular solid model and the computer aided design (CAD) model. In this paper, a new framework is proposed to achieve a 3D printing vascular model with high simulation. The patient-specific 3D reconstruction of the coronary arteries is performed by the detailed morphological information abstracted from the contour of the vessel lumen. In the process of reconstruction which has 5 steps, the morphological details of the contour view of the vessel lumen are merged along with the curvature and length information provided by the coronary angiography. After comparing with the diameter of the narrow section and the diameter of the normal section in CAD models and 3D printing model, it can be concluded that there is a high correlation between the diameter of vascular stenosis measured in 3D printing models and computer aided design models. The 3D printing model has high-modeling ability and high precision, which can represent the original coronary artery appearance accurately. It can be adapted for prevascularization planning to support doctors in determining the surgical procedures.

1. Introduction

With the fast development of the society, China's basic medical care has been well improved. However, the prevalence and mortality of cardiovascular diseases (CVD) in residents is still rising, and which in recent years rapidly

grow for the low-aged and low-income citizens. Since 2004, the rate of hospitalization of cardiovascular diseases is much faster than the growth rate of GDP, greatly increasing the social burden [1–3]. CVD mainly include cerebrovascular disease, coronary heart disease, arrhythmia, and heart failure. CVD has become the largest proportion of residents

suffering from all disease; 2 out of every 5 deaths are due to cardiovascular diseases. Since 2009, CVD mortality rate in rural regions has exceeded and continues to be above urban levels. In 2015, the CVD mortality rate of rural residents was 298.42/100,000, of which the heart disease mortality rate was 144.79/100,000, the cerebrovascular disease mortality rate was 153.63/100,000, and the urban residents' CVD mortality rate was 264.84/100,000, including heart disease death. The rate was 13.661/100,000, and the mortality rate of cerebrovascular disease was 128.23/100,000. In 2015, the proportion of CVD deaths in rural and urban residents accounted for 45.01% and 42.61%, respectively. Thus, it is imperative to early diagnose cardiovascular disease [1].

There are two methods being widely used in the detection of cardiovascular diseases, namely, OCT technology and coronary angiography. Optical coherence tomography (OCT) technology is an imaging technique that uses near-infrared light to display the associated tissue structure in the blood vessels without radiation, high resolution, and high-detection sensitivity [4, 5]. OCT can perform high-resolution cross section tomography images of biological tissue endometrium and provide a resolution ten times higher than intravascular ultrasound, so it is also called optical biopsy. On the basis of the first-generation time domain OCT (TD-OCT) system, scientists developed frequency domains with faster scanning speeds by varying the frequency of light to obtain different depth tissue imaging OCT (frequency domain OCT, FD-OCT) system [6]. X-ray coronary angiography is an arterial angiography method using an angiography machine. The procedures are as follows: first, through a special cardiac catheter percutaneous puncture, a special catheter is inserted through the right iliac artery or the lower extremity femoral artery, and the descending aorta is retrogradely to the ascending aorta root. Then, the left or right coronary artery is inserted and injected with the contrast agent. Eventually, the coronary artery and morphological are visible. X-ray coronary angiography can clearly distinguish the location and morphological characteristics of vascular lesions, quantitatively determine and classify narrow vascular segments, and determine the circulation state of lateral branches [7]. However, the technology itself has certain limitations. Firstly, it can only display the projection of the lumen of the blood vessel and not the cross-sectional information of the tube wall, which may cause the doctor to miss the diagnosis; secondly, it cannot provide information on the morphology and properties of plaques, and it is thus impossible to develop interventional procedures for specific plaque information; lastly, because of the uneven filling of the contrast agent in the blood vessels, it is easy for the doctor to underestimate the degree of lumen narrowing.

In response to the limitations of the above two technologies, we introduced 3D printing technology. Three-dimensional (3D) printing technology, also known as additive manufacturing technology, has advantages of fast, directness, and digitalize. [8] Since its appearance in the 1980s, 3D printing technology has developed rapidly in this century and has been widely used in the fields of automobile, aerospace, and medical. It can be applied to enhance the

diagnosis and treatment of complex cardiovascular diseases, allowing doctors to visually evaluate the spatial geometry of the entire vessel [9]. The appearance of rapid prototyping techniques (RPT) greatly made the computer technology move forward, and 3D printing is one type of the RPT [10]. A rapid 3D prototyping process consists of many steps. This technique needs to obtain a series of figures, such as computed tomography (CT) images, transform the figures into a format compatible with a 3D printer, and then print the model [11]. Some surgeries can be planned using three-dimensional computer aided design and manufacturing (3D CAD/CAM) software. The 3D virtual planning is performed in PROPLAN software and exported into 3-matic software to design and then use the biocompatible material to print [12]. Shaheen et al. and Rengier and Mehndiratta used dedicated postprocessing algorithm to extract a spatial model from image data sets and export to machine-readable data [12, 13].

At present, there are few research studies on 3D printing of coronary arteries. This paper explores the 3D printing of blood vessels based on optical coherence tomography and coronary angiography. Angiographic images and optical coherence tomography images of 8 patients with coronary artery stenosis before and after implantation of stents were collected. The vascular model of the eight patient models were modeled with the proposed 3D reconstruction technique by merging the morphological details of the contour view of the vessel lumen and the curvature and length information provided by the coronary angiography. After outputting the STL file format, the built-in coronary STL format file is then imported into the 3D printer and the STL format file is converted into a machine code Gcode that can be recognized by the 3D printer. Finally, the 3D printer performs coronary artery model printing operation. The main contribution of the paper is to originally complete the 3D printing of specific blood vessel models with high correlations between the diameters of the vascular stenosis segments extracted from the 3D reconstruction model.

Compared with the traditional scheme, our new approach has advantages of high-quality simulation, applicability in clinical usages, and the convenience of preoperative planning.

2. Methods

The overall flowchart of our proposed framework with 5 steps is shown in Figure 1, where 5 steps are mainly contained. The original images are preprocessed and the used for reconstructing the 3D solid model of the blood vessel. And then the 3D point clouds are extracted from biodegradable stent, which are introduced to the reconstruction of the 3D solid model of the bioabsorbable stent. Finally, the 3D solid model of the blood vessel after implantation of the bioabsorbable stent is reduced through feature subtraction.

2.1. Individualized Three-Dimensional Reconstruction of Coronary Arteries. The individualized 3D reconstruction of the coronary arteries is performed by merging the

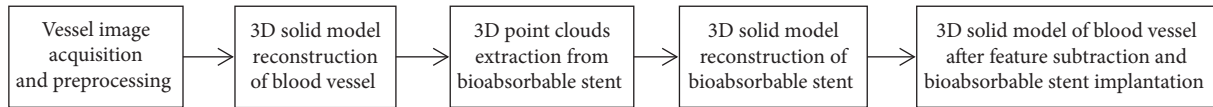


FIGURE 1: The flowchart of our proposed framework on patient-specific coronary artery 3D printing.

morphological details of the contour view of the vessel lumen and the curvature and length information provided by the coronary angiography. We first performed a three-dimensional reconstruction with coronary angiography containing information on vessel curvature and high-resolution intravascular optical coherence tomography. The reconstruction steps include blood vessel image acquisition and preprocessing, reconstruction of a 3D vascular solid model, extraction of a 3D point cloud of a biodegradable stent, reconstruction of a 3D solid model of the biodegradable stent, [14] and reduction of the feature after subtraction of the implanted bioabsorbable stent of the 3D solid model of blood vessels [15]. The following are a specific description of the various steps of the reconstruction.

2.1.1. Step 1: Acquire and Preprocess the Vascular Image.

The central line of vascular structure was extracted according to the coronary angiography image. According to the number of framing pictures of the intravascular OCT image, evenly divide the center line to obtain a series of points and set a plane perpendicular to the center line at each point.

2.1.2. Step 2: Rebuild the Three-Dimensional Vascular Solid Model.

Each frame is placed in the corresponding plane in order from the IVOCT image sequence, the contour of the lumen is identified, and the image is removed after the contour is obtained. Repeat the above steps for each image until the skeleton corresponding to the contour of the entire vessel lumen is achieved, select the contours of each vascular cavity, perform a sweep operation along the centerline of the coronary angiography, and smooth the surface of the 3D blood vessels to eventually produce a vascular solid model [16]. Figures 2(a)–2(c) represent the process of modeling a 3D model of blood vessels.

2.1.3. Step 3: Extract the Three-Dimensional Point Cloud of Biological Absorbable Stent.

For the vessel segment implanted with the stent column, firstly, according to the automatic stent extraction algorithm proposed in Figure 3, each stent column point is displayed at the position of the IVOCT per frame. When all the scaffold points are automatically marked, a discrete 3D scaffold point cloud is obtained. The position of the point cloud is the position of the scaffolding column in the IVOCT chart of each frame. The geometrical space structure of the support can be approximately obtained by the support point cloud.

2.1.4. Step 4: Three-Dimensional Solid Model for Reconstruction of Biological Absorbable Stents.

After building the

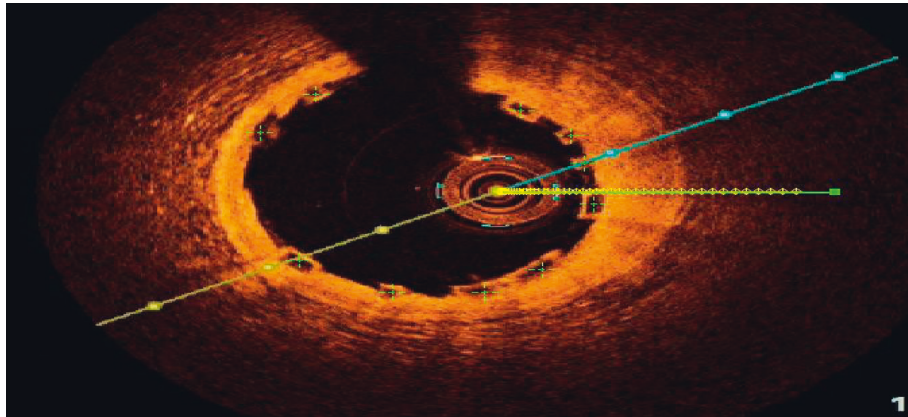
bracket point cloud, in order to restore the mesh structure of the bracket, we also need to manually connect the bracket columns to construct the spatial structure of the biological absorbable stent in the vascular cavity. According to the prior information, we know that the bracket is made up of annular structures, each of which is connected by a scaffold [17, 18]. According to the observation, we found that the distance of every 3 to 4 OCT frames is the thickness of a mesh bracket ring, and the structure of the stent-ring can be generated by sequentially connecting the point cloud of the stent column in the adjacent 3 to 4 frames of IVOCT by a curve. Since the bracket is thick, we first calculate the diameter of the bracket column according to the OCT picture. Then, a new plane is established on the plane perpendicular to the ring curve of the bracket, centered on the intersection of the surface and the plane, and a circle is drawn in diameter with the thickness of the precalculated bracket column. For each annular structure of the stent, the circle is swept along the curve of the stent ring to create a ring-shaped stent body having a thickness. The three-dimensional point cloud and its 3D model of the bracket are illustrated in Figures 4(a) and 4(b).

2.1.5. Step 5: Three-Dimensional Solid Model of Blood Vessels after Reduction and Implantation of Biologically Absorbable Stents upon Feature Subtraction.

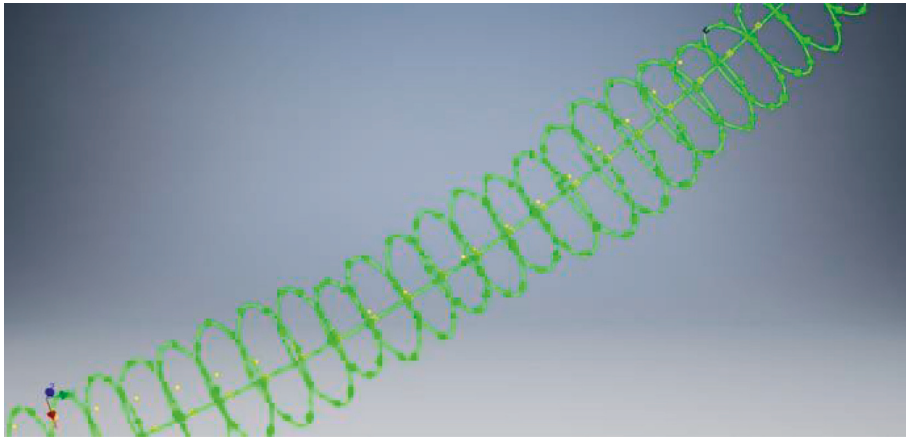
For the vessel segment implanted in the stent, we subtract the feature of the generated vascular entity from the bioabsorbable stent entity, forming a stent groove on the modeled vascular entity to highlight the stent structure, and restore the real 3D vascular cavity structure with the stent placed [19]. A 3D vascular model of an implanted biological absorbable stent with a corrugated surface is shown in Figures 5(a) and 5(b).

2.2. Exploration of Three-Dimensional Printing Specific Vascular Model.

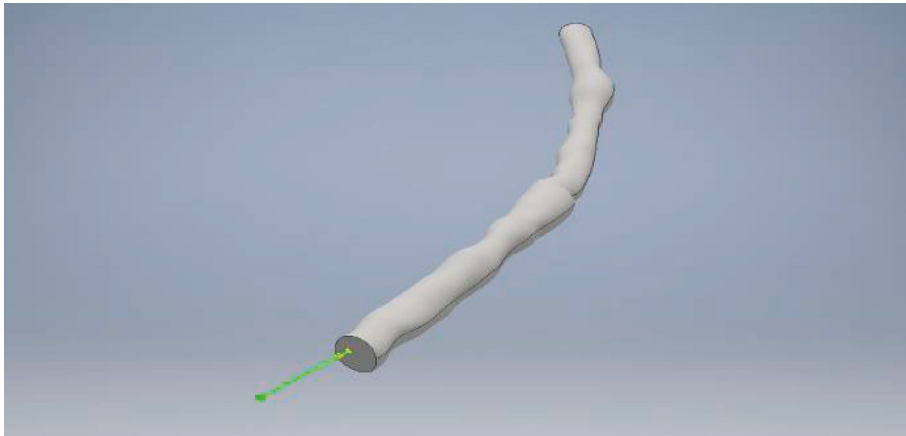
The application of 3D printing in medicine has changed the limitation that traditional 3D models can only be virtual displayed on computers. Doctors can make more accurate preoperative planning and improve the success rate of surgery by analyzing the anatomical structure characteristics of lesions through personalized medical model entity. At present, clinicians mainly design the operation plan based on CT, MRI, angiography, or 2D vascular lumen images such as optical coherence tomography, vascular ultrasound images, and clinical experience. However, these imaging techniques can only present two-dimensional field of vision on the screen and cannot allow doctors to visualize the spatial geometry of the whole blood vessel evaluation [20]. 3D printing technology can be applied to the diagnosis and treatment of complex cardiovascular diseases. The 3D model of coronary artery can facilitate physicians to



(a)



(b)



(c)

FIGURE 2: (a–c) Fusion IVOCT and CAG images of vascular three-dimensional model reconstruction.

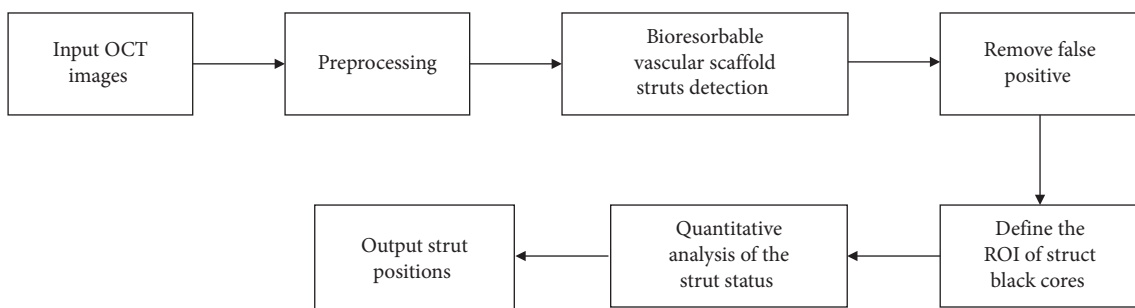


FIGURE 3: Flowchart of the automatic stent extraction algorithm.

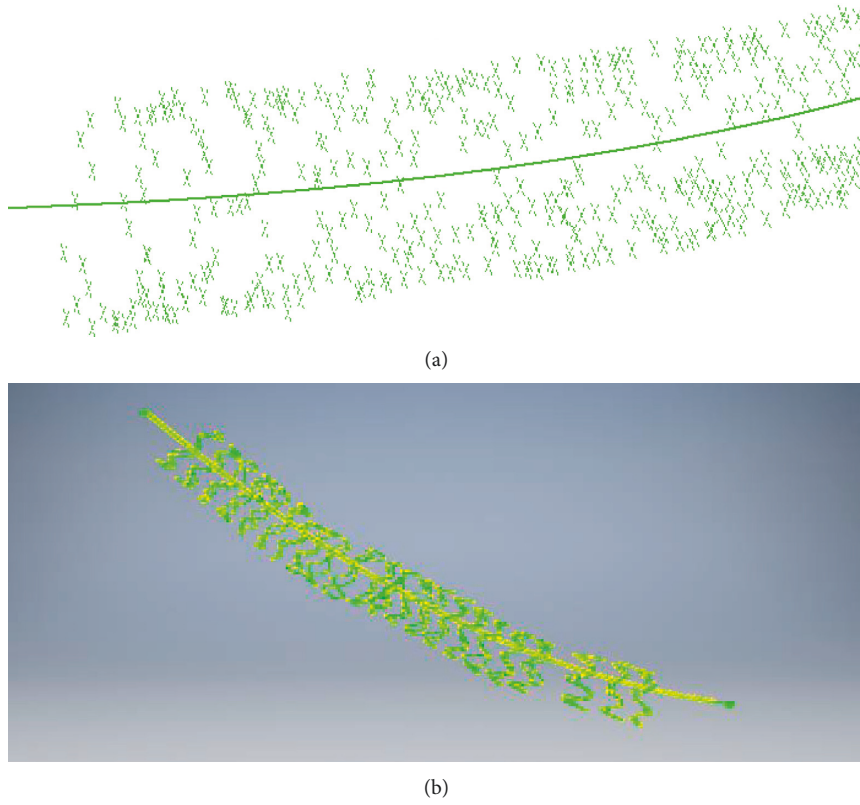


FIGURE 4: (a) Biodegradable scaffold point cloud extraction. (b) Three-dimensional model reconstruction.

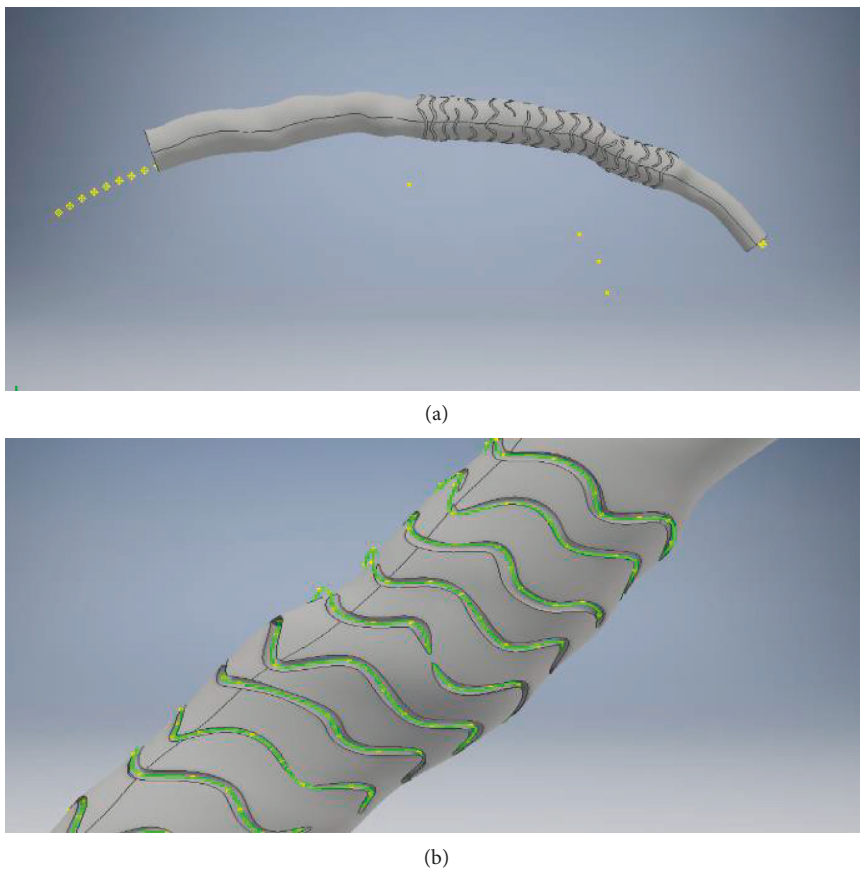


FIGURE 5: A three-dimensional model of a bioabsorbable stent with a corrugated surface (a) obtained by subtracting the three-dimensional model of the vessel from the stent (b).

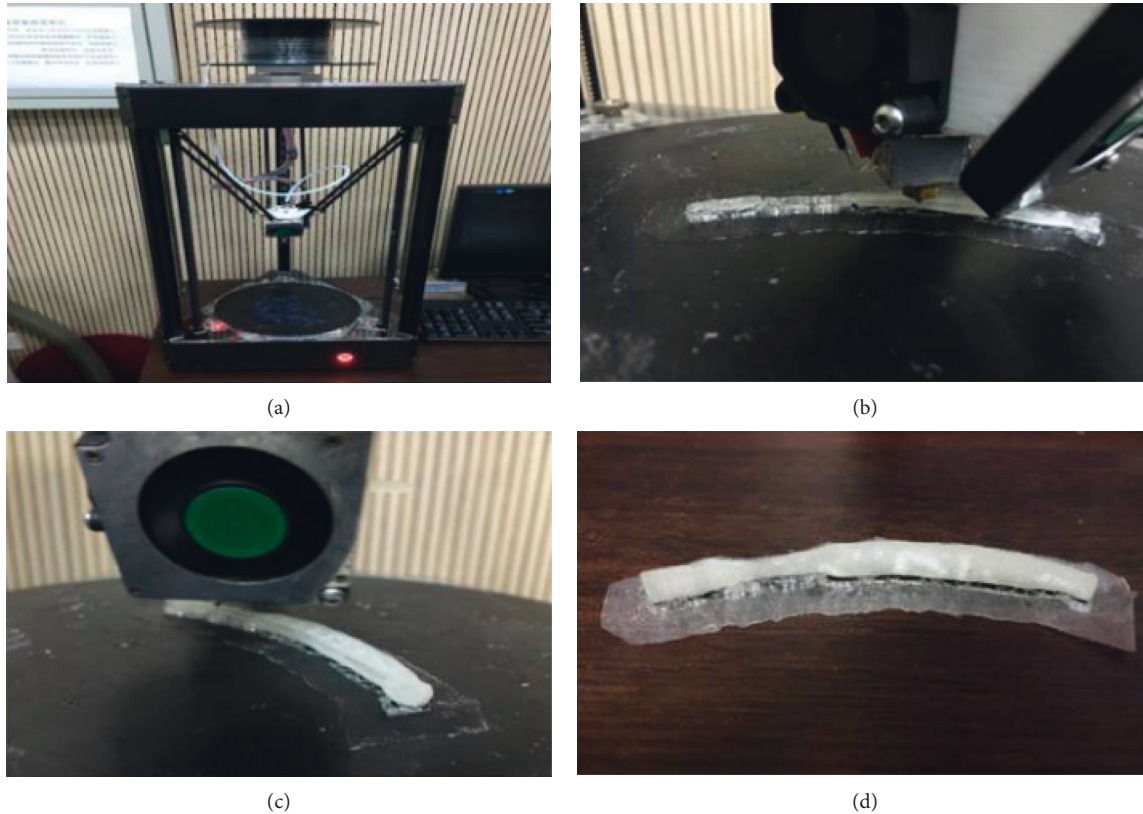


FIGURE 6: The process of 3D printing a specific vascular model.

intuitively touch and measure the pathological vascular segments, so as to determine the key steps of operation, select the appropriate size of vascular branches, and formulate the best surgical plan, which can reduce the possibility of uneven stent adherence and hence greatly improve the effectiveness of interventional surgery [21, 22].

The individual geometry of lesions in each branch of coronary artery varies greatly and the treatment scheme is more complex, especially in the selection of stents and implantation location of interventional surgery. In this paper, we attempt to explore the spatial geometry of the coronary artery by using 3D printing technology. Through individualized 3D reconstruction of the coronary artery, we have successfully obtained 3D vascular model structure. The structure of the 3D model is expected to change the situation in which clinicians perceive coronary artery lesions based on their own experience in the past. Quantitative experimental results also show that the 3D printing technology has high visualisation quality and the effectiveness of the 3D model of the coronary artery in individualized coronary intervention surgery and preoperative planning.

3. Experiment

In this study, we collected angiographic images and optical coherence tomography images of 8 patients with coronary artery stenosis before and after implantation of stents. 3D modeling of the vascular model of 8 patients was performed

using the proposed 3D reconstruction technique and the STL file format was output.

By analyzing the advantages and disadvantages of common 3D printing technology, this study selects a 3D printer based on melting deposition molding technology to carry out the research on the geometrical morphological structure of the coronary artery. Considering that the coronary artery vascular model is very small, in order to be able to observe the structural differences of different vascular models more intuitively by the printing vascular model, we first performed a 2x scale morphological enlargement of the vessel 3D model. In this work, we selected the fused deposition 3D printer of EasyArts's model areas and picked polylactic acid as the printing material [4]. The parameters of the device are X , Y , and Z in the direction of the accuracy of 0.02 mm and the maximum printable size of $160 * 160 * 160$ mm. When printing, the thickness of each layer is 0.05–0.3 mm, the nozzle size is 0.3 mm, and the nozzle temperature heating range is 170–280 degrees Celsius.

After importing the coronary STL format file into the 3D printer, the first step is to check the STL format file. The original model may have some minor flaws in modeling, and in order to make the model more complete, we need to check the integrity of the STL model and then fill, smooth, rotate, zoom, and so on as needed. Convert the STL format file to a machine code Gcode that can be recognized by a 3D printer, which generates a print backplane, print support, and other



FIGURE 7: Measuring process using a vernier caliper.

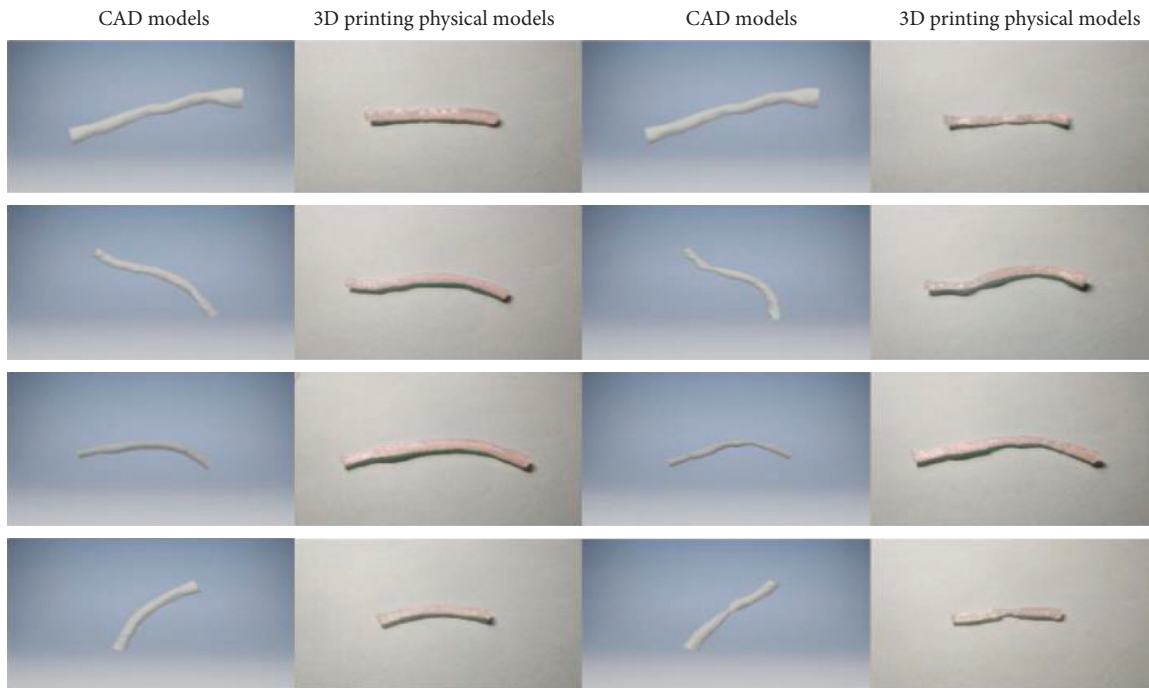


FIGURE 8: Comparison of 8 selected coronary artery CAD models and 3D printing physical models.

operations based on the model structure. 3D printer performs coronary artery model printing operations. Under the control of the computer, the nozzle moves along the xy plane and the molten wire in the semiflowing state is squeezed out of the nozzle, coated on the workbench, and cooled to form a cross section. After a layer of molding, the nozzle moves up a layer of height and is stacked according to this reciprocating operation to form a 3D entity until the end of the print.

4. Results

The postprocessing step includes the removal of support, surface polishing, and other operations.

Finally, a smooth 3D printing vascular model entity was achieved as shown in Figure 6.

The diameter of the printing coronary artery solid stenosis section and the diameter of the normal segment were measured using a vernier caliper (Figure 7) and compared with the diameter of the narrow section and the diameter of the normal section in the 3D model of the coronary artery in the software.

Comparison of 8 cases of the coronary artery CAD model and 3D printing physical model is shown in Figure 8.

Figure 8 shows that the diameter of the printing coronary artery solid stenosis section and the diameter of the normal segment were measured using a vernier caliper and compared with the diameter of the narrow section and the diameter of the normal section in CAD models. And a series of measurements are included from Figures 9–11. It can be seen that the diameter of the stenosis segment measured in the 3D printing model is highly correlated with the diameter of the stenosis segment extracted from the CAD models. Table 1 shows that 3D printing models and CAD models of 3D measurements in stenosis and nonstenosis coronary artery segment.

The source of vascular data is rich, including coronary angiography, using X-ray acquisition, intravascular ultrasound images acquired with ultrasound techniques, intravascular optical coherence tomography images acquired via optical correlation tomography, and magnetic resonance angiography and computed tomography images. Vascular data not only preserves the information on the surface of

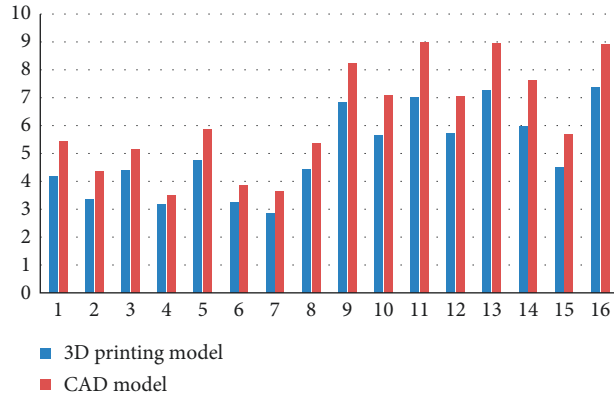


FIGURE 9: Measurement results of 3D printing models and CAD models.

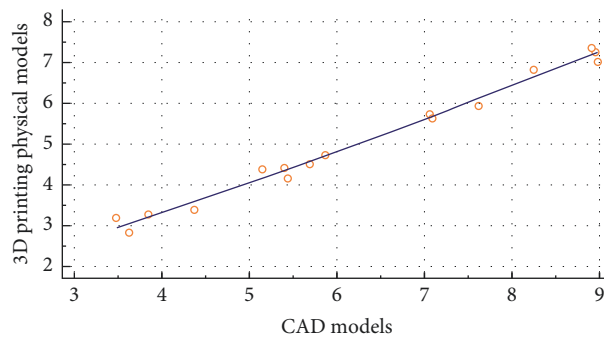


FIGURE 10: Correlation of the diameter of the stenosis segment measured in the 16 3D printing models and CAD models.

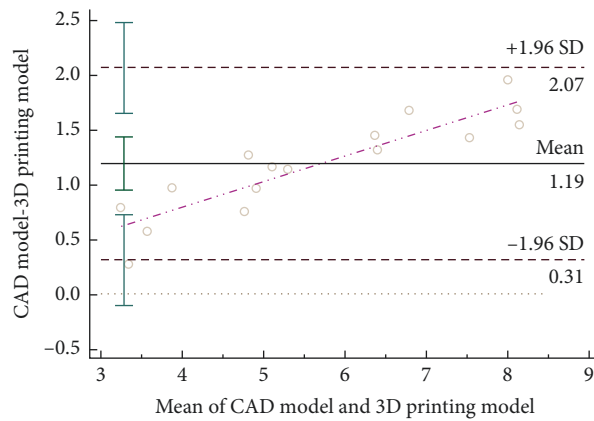


FIGURE 11: Bland-Altman plot for the 3D printing models and CAD models.

blood vessels but also contains abundant information on the internal structure of blood vessels, which is beneficial to the imaging diagnosis of related cardiovascular diseases in clinic [23, 24]. However, the above imaging technology can only present a two-dimensional field of vision on the screen and cannot permit doctors to intuitively evaluate the spatial geometry of the whole blood vessel [25].

3D printing of vascular technology in the diagnosis and treatment of cardiovascular diseases has a very important application value, we believe that this technology has the following two main advantages. (1) High quality of simulation: experimental studies have shown that the 3D printing

vascular technology has high simulation ability and can accurately model the specific blood vessels of patients. The printing solid model is sufficient for general clinical application needs and can help doctors better understand the details of blood vessels. (2) Preoperative planning: the 3D model of coronary arteries facilitates the planning of preoperative planning for vascular implantation [26]. The manifested vascular model can accommodate the visual touch of the cardiologist and measure the vascular segment of the lesion, so as to determine the key steps of the operation, select the appropriate size of the blood vessel branch, develop the best surgical scheme, reduce the

TABLE 1: 3D printing physical models vs CAD models of 3D measurements of blood vessels in stenosis and nonstenosis.

| Number | 3D printing models | | | | CAD models | | | |
|--------|---------------------|--------------------|---------------------|--------------------|---------------------|--------------------|---------------------|--------------------|
| | Stenosis (mm) | | Nonstenosis (mm) | | Stenosis (mm) | | Nonstenosis (mm) | |
| | Before implantation | After implantation | Before implantation | After implantation | Before implantation | After implantation | Before implantation | After implantation |
| 1 | 4.17 | 6.82 | 7.03 | 7.02 | 5.44 | 8.25 | 8.42 | 8.81 |
| 2 | 3.39 | 5.64 | 5.68 | 5.94 | 4.37 | 7.09 | 7.28 | 7.24 |
| 3 | 4.39 | 7.02 | 8.22 | 8.54 | 5.15 | 8.98 | 9.70 | 10.18 |
| 4 | 3.20 | 5.74 | 6.55 | 6.38 | 3.48 | 7.06 | 7.65 | 8.61 |
| 5 | 4.73 | 7.26 | 7.76 | 7.93 | 5.87 | 8.95 | 9.83 | 9.67 |
| 6 | 3.27 | 5.94 | 6.36 | 6.86 | 3.85 | 7.62 | 8.09 | 8.55 |
| 7 | 2.84 | 4.52 | 6.18 | 5.38 | 3.63 | 5.69 | 7.91 | 7.22 |
| 8 | 4.42 | 7.36 | 8.70 | 9.08 | 5.40 | 8.91 | 10.09 | 9.85 |

possibility of stent adherence unevenness, and greatly improve the effectiveness of interventional surgery [27]. At the same time, due to the stability of the printing material, the solid model can also be viewed and carried by doctors at any time [28].

5. Conclusion

In this paper, a new framework is proposed to print a 3D vascular model with a high simulation value. Experimental results conclude that the 3D printing vascular model based on OCT and angiography has a high correlation with the vascular 3D reconstruction model. The 3D vascular model we printed has the characteristics of high simulation, applicability in clinical application, and the convenience of preoperative planning, which has obvious advantages as compared with the traditional scheme. It also gives a new scheme for the treatment of cardiovascular diseases, which has extremely high practical significance and good application prospects. In the future, the following 3 aspects need to be improved further: (1) the currently printing vascular model is a solid entity and it is not possible to print a cavity vessel, and it is impossible to perform a simulated interventional procedure. (2) The currently printing material is polylactic acid, which is quite hard to read compared to vascular tissue. (3) The time of making the blood vessel model is still relatively long, and the manual deburring is required in the later stage, where the automaticity needs to be improved.

Data Availability

The data used to support the findings of this study are available from the corresponding author upon request.

Conflicts of Interest

The authors declare that they have no conflicts of interest.

Acknowledgments

This work was supported in part by the National Science and Technology Support Program under Grant 2015BAF10B01 and Natural Science Foundation of China under Grants 81670403, 81500381, and 81201069.

References

- [1] W. Chen, R. L. Gao, L. S. Liu et al., "Summary of China cardiovascular disease report 2017," *China Circulation Magazine*, vol. 33, no. 1, pp. 1–8, 2018.
- [2] C. Huang, Y. Xie, Y. Lan et al., "A new framework for the integrative analytics of intravascular ultrasound and optical coherence tomography images," *IEEE Access*, vol. 6, pp. 36408–36419, 2018.
- [3] C. Huang, X. Shan, Y. Lan et al., "A hybrid active contour segmentation method for myocardial D-SPECT images," *IEEE Access*, vol. 6, pp. 39334–39343, 2018.
- [4] H. Lu, M. Garghesha, Z. Wang et al., "Automatic stent strut detection in intravascular OCT images using image processing and classification technique," *Proceedings of SPIE-The International Society for Optical Engineering*, vol. 8670, p. 15, 2013.
- [5] C. Huang, G. Tian, Y. Lan et al., "A new pulse coupled neural network (PCNN) for brain medical image fusion empowered by shuffled frog leaping algorithm," *Frontiers in Neuroscience*, vol. 13, pp. 1–10, 2019.
- [6] K. P. Tung, W. Z. Shi, L. Pizarro et al., "Medical imaging 2012: computer-aided diagnosis-automatic detection of coronary stent struts in intravascular OCT imaging," in *Proceedings of the SPIE Medical Imaging*, San Diego, CA, USA, February 2012.
- [7] B. Ripley, T. Kelil, M. K. Cheezum et al., "3D printing based on cardiac CT assists anatomic visualization prior to transcatheter aortic valve replacement," *Journal of Cardiovascular Computed Tomography*, vol. 10, no. 1, pp. 28–36, 2015.
- [8] B. Berman, "3-D printing: the new industrial revolution," *Business Horizons*, vol. 55, no. 2, pp. 155–162, 2012.
- [9] C. Colasante, Z. Sanford, E. Garfein, and O. Tepper, "Current trends in 3D printing, bioprosthesis, and tissue engineering in plastic and reconstructive surgery," *Current Surgery Reports*, vol. 4, no. 2, p. 6, 2016.
- [10] M. Mcgurk, A. A. Amis, P. Potamianos, and N. M. Goodger, "Rapid prototyping techniques for anatomical modelling in medicine," *Annals of the Royal College of Surgeons of England*, vol. 79, no. 3, pp. 169–174, 1997.
- [11] J. D. Wagner, B. Baack, G. A. Brown, and J. Kelly, "Rapid 3-dimensional prototyping for surgical repair of maxillofacial fractures: a technical note," *Journal of Oral and Maxillofacial Surgery*, vol. 62, no. 7, pp. 898–901, 2004.
- [12] E. Shaheen, Y. Sun, R. Jacobs, and C. Politis, "Three-dimensional printing final occlusal splint for orthognathic surgery: design and validation," *International Journal of Oral and Maxillofacial Surgery*, vol. 46, no. 1, pp. 67–71, 2017.
- [13] F. Rengier, A. Mehndiratta, H. von Tengge-Kobligk et al., "3D printing based on imaging data: review of medical

- applications,” *International Journal of Computer Assisted Radiology and Surgery*, vol. 5, no. 4, pp. 335–341, 2010.
- [14] W.-X. Fu, Q. Wang, Y. S. Zhang et al., “Application of ultrasound technology in the diagnosis and treatment of digestive tract diseases,” *European Review for Medical and Pharmacological Sciences*, vol. 19, no. 4, pp. 602–606, 2015.
- [15] L. Chen, *3D Printing Aneurysm Model and Simulated Surgical Approach*, Hebei Medical University, Shijiazhuang, China, 2017.
- [16] W. Ben, R. J. Mobbs, A.-M. Wu, and K. Phan, “Systematic review of 3D printing in spinal surgery: the current state of play,” *Journal of Spine Surgery (Hong Kong)*, vol. 3, no. 3, pp. 433–443, 2017.
- [17] B. Jeon, C. Lee, M. Kim, T. H. Choi, S. Kim, and S. Kim, “Fabrication of three-dimensional scan-to-print ear model for microtia reconstruction,” *Journal of Surgical Research*, vol. 206, no. 2, pp. 490–497, 2016.
- [18] K. M. Meess, R. L. Izzo, M. L. Dryjski et al., “3D printing abdominal aortic aneurysm phantom for image guided surgical planning with a patient specific fenestrated endovascular graft system,” *Proceedings of SPIE-The International Society for Optical Engineering*, vol. 10138, 2017.
- [19] J. R. Anderson, W. L. Thompson, A. K. Alkattan et al., “Three-dimensional printing of anatomically accurate, patient specific intracranial aneurysm models,” *Journal of Neuro-Interventional Surgery*, vol. 8, no. 5, pp. 517–520, 2016.
- [20] M. Markl, R. Schumacher, J. Küffer, T. A. Bley, and J. Hennig, “Rapid vessel prototyping: vascular modeling using 3t magnetic resonance angiography and rapid prototyping technology,” *Magnetic Resonance Materials in Physics, Biology and Medicine*, vol. 18, no. 6, pp. 288–292, 2005.
- [21] Z. Wang, M. W. Jenkins, G. C. Linderman et al., “3-D stent detection in intravascular OCT using a bayesian network and graph search,” *IEEE Transactions on Medical Imaging*, vol. 34, no. 7, pp. 1549–1561, 2015.
- [22] H. S. Nam, C.-S. Kim, J. J. Lee, J. W. Song, J. W. Kim, and H. Yoo, “Automated detection of vessel lumen and stent struts in intravascular optical coherence tomography to evaluate stent apposition and neointimal coverage,” *Medical Physics*, vol. 43, no. 4, pp. 1662–1675, 2016.
- [23] G. Unal, S. G. S. Gurmeric, and S. G. Carlier, “Stent implant follow-up in intravascular optical coherence tomography images,” *The International Journal of Cardiovascular Imaging*, vol. 26, no. 7, pp. 809–816, 2010.
- [24] S.-J. Yoo, T. Spray, E. H. Austin, T.-J. Yun, and G. S. van Arsdell, “Hands-on surgical training of congenital heart surgery using 3D print models,” *The Journal of Thoracic and Cardiovascular Surgery*, vol. 153, no. 6, pp. 1530–1540, 2017.
- [25] A. Liu, G.-H. Xue, M. Sun et al., “3D printing surgical implants at the clinic: a experimental study on anterior cruciate ligament reconstruction,” *Scientific Reports*, vol. 6, no. 1, p. 21704, 2016.
- [26] P. Weinstock, S. P. Prabhu, K. Flynn, D. B. Orbach, and E. Smith, “Optimizing cerebrovascular surgical and endovascular procedures in children via personalized 3D printing,” *Journal of Neurosurgery: Pediatrics*, vol. 16, no. 5, pp. 584–589, 2015.
- [27] A. Braga, P. Mora, and A. C. de Melo, “Challenges in the diagnosis and treatment of gestational trophoblastic neoplasia worldwide,” *World Journal of Clinical Oncology*, vol. 10, no. 2, pp. 28–37, 2019.
- [28] J. Ni, D. Li, M. Mao et al., “A method of accurate bone tunnel placement for anterior cruciate ligament reconstruction based on 3-dimensional printing technology: a cadaveric study,” *Arthroscopy: The Journal of Arthroscopic & Related Surgery*, vol. 34, no. 2, pp. 546–556, 2018.

